FROM: Crossing Bridges: Advances in Flexible Automation and Robotics
Proceedings of the USA-JAPAN Symposium on Flexible Automation, July 18-20, 1988
Minneapolis, MN, USA.

DYNAMIC ANALYSIS AND CONTROL OF LIGHTWEIGHT ARMS WITH A PARALLEL MECHANISM

B. -S. Yuan, J. W. Lee, and W. J. Book
The George W. Woodruff School of Mechanical Engineering
Georgia Institute of Technology
Atlanta, Georgia

ABSTRACT

A parallelogram drive enables lightweight arms to have a higher rigidity and to reduce the actuator weight moved. Analysis of the flexible closed kinematic chain dynamics and design of the control are described in this paper. The system dynamics is derived by the Lagrangian formula via the assumed mode method. Holonomic constraints due to the geometry of the parallelogram mechanism must be imposed on the dynamics. An orthonormal basis has been computed from the singular value decomposition of the constraint Jacobian matrix in order to eliminate the constraint force in the equations of motion. The comparatively large workspace and fast motion make motion control with flexibility in each link computationally demanding. The general rigid control (GRC) is implemented to overcome these problems. The solution algorithm checks the constraint violations. Numerical simulation illustrates the results under feedback control.

I. INTRODUCTION

A large scale robot system has many useful applications, such as material handling, assembling an aircraft and space operation. Traditionally, robot manipulators have been designed for rigidity with short arm length and heavy construction. This approach may not be applicable to large structures. Therefore, an alternative approach utilizing lightweight materials for the robotic system is highly desirable [1,4]. In exchange for lightweight, one must accept an increase in system flexibility along with the associated difficulty in accurately controlling a flexible structure [2,3]. To counteract this lack of rigidity, a parallel kinematic chain is included in the robot structure instead of a purely serial-link design. The advantages of a parallelogram drive mechanism are higher rigidity, higher load capacity and lower interactive forces between links.

A dynamic model for serial-link flexible arms has been developed using Lagrange's equations, with the link deflection expressed by the assumed mode method [5]. This method will be extended to a parallel mechanism with flexible links by choosing the joint coordinate frames properly, and including the workless force attributed to the geometric constraints [6]. However, many algorithms have been proposed to solve the constrained dynamics [7]. Some solve the equation of motion and constraints simultaneously by determining the constraint force in terms of the Lagrange multiplier [8]. Others use a reduction method that eliminates the constraint forces explicitly from the equation of motion [9,10,15]. In this paper, the singular value decomposition (SVD) is imposed to reduce the constrained dynamic systems to their minimum dimension. Furthermore, the constraint Jacobian matrix is decomposed into independent coordinate and dependent coordinate sets so that all system information associated with the independent coordinates can be derived and a transformation back to the physical coordinate obtained.

The constraint forces may not be directly controlled, but one can maintain the constraint force invariant in small motion [11]. However, fast motion and large working area are desirable for designing a large-scale robot. System vibration due to the flexibility in each link of the lightweight structure also needs to be considered during motion control [12]. One way which meets those requirements is to choose the independent joint control (IJC) [17]. However, the general rigid control (GRC) is implemented here to improve performance with an increase in complexity.

Finally, the numerical algorithm is used to solve the responses of the constrained equation of motion and demonstrate the effectiveness of the method.

II. DYNAMIC MODELING

The schematic drawing of a two link manipulator, **RALF** (Robotic Arm, Large Flexible), with a parallel mechanism existing in the Flexible Automation Laboratory at Georgia Tech is shown in Fig. 1 [14]. The structure consists of two 3m long links and a parallel actuating link. In order to analyze the motion of the system, the position of every point along the structure needs to be specified by coordinate systems as in Fig. 2. The flexible deflection $W_i(x,t)$ of each link i relative to a rigid-body rotation is assumed to be a linear combination of vibratory modes [5];

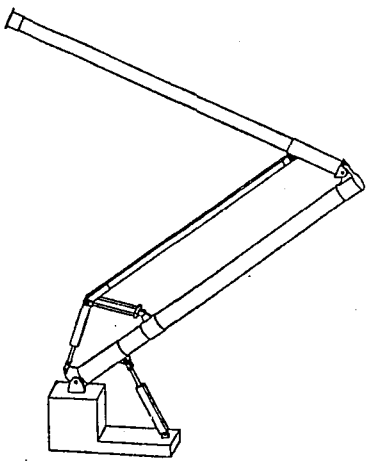

Figure 1. The two RALF with a parallel mechanism.

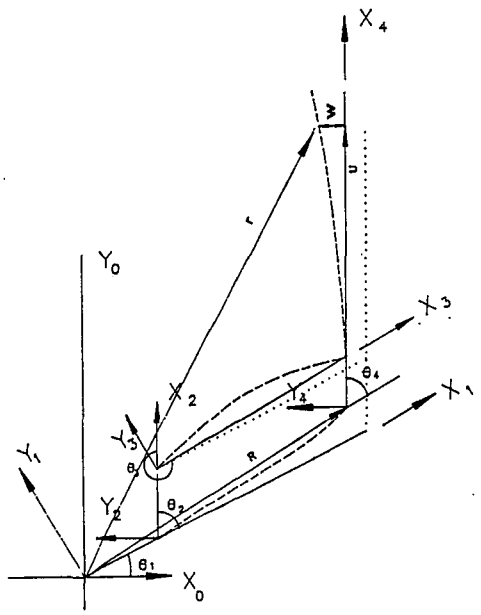

Figure 2. Coordinate Systems for the assumed mode method.

$$W_i(x,t) = \sum_{j=1}^{l} \xi_{ij}(x)\ \eta_{ij}(t) \qquad (2\text{-}1)$$

where $\xi_{ij}(x)$ is an admissible shape function and $\eta_{ij}(t)$ is a time-dependent generalized coordinate. $W_i(x,t)$ should satisfy the Bernoulli-Euler beam equation [13]

$$EI\ \frac{\partial^4 W_i}{\partial x^4} + \frac{\partial^2 W_i}{\partial t^2} = 0 \quad , \qquad (2\text{-}2)$$

where EI = Flexural Rigidity. The shape function $\xi(x)$, is determined by the boundary conditions and greatly influences the results of the dynamic model. The boundary conditions are therefore chosen carefully for each link. According to the initial experiments [14], the boundary conditions are clamped-free for the upper link, clamped-mass for the lower link, and pin-pin for the parallel actuating link. The generalized coordinate $\eta(t)$ can be treated as state variable in the state-space formulation.

Geometrically, the absolute position vector $\vec{r}_i$ of an arbitrary point on each link i is composed of rigid and elastic generalized components,

$$\vec{r}_i = \vec{R}_i + \vec{u}_i + \vec{W}_i \qquad (2\text{-}3)$$

where $\vec{R}_i$ is the position vector to the origin of the reference coordinate measured with respect to the base frame, and $\vec{u}_i$ is the undeformed position of each link.

Next, one constructs the kinetic and potential energies for each link to compute the Lagrangian. Due to the distributed character of the flexible link, the kinetic energy $(K.E.)_i$ is taken into account by integrating over each link i

$$(K.E.)_i = 1/2 \int_0^{L_i} \dot{\vec{r}}_i \cdot \dot{\vec{r}}_i\ dm \quad i=1,3,4 \qquad (2\text{-}4)$$

where L_i is the length of the link i. The potential energy of link i, $(P.E.)_i$, due to link elasticity is accounted for by the modal stiffness K_{ij}

$$K_{ij}\ \ (EI)_i \int_0^{L_i} \xi''_{ij}(x)\ dx \quad i = 1,3,4 \qquad (2\text{-}6)$$

$$(P.E.)_i = \frac{1}{2} \sum_{j=1}^{l} K_{ij}\eta_{ij}^2(t) \qquad (2\text{-}7)$$

The closed chain of this structure can be separated into two open trees with an unknown constraint force acting on them. The separation point is chosen here at the joint between the upper and the parallel links as indicated in Fig. 1. Therefore, the motion of the system is constrained by a set of m holonomic constraint equations and does not depend explicitly upon time; i.e.

$$\Phi(q) = 0 \qquad (2\text{-}8)$$

where q is a vector consisting of $[\theta, \eta]^T$, and $\theta = [\theta_1,..,\theta_4]^T$, $\eta = [\eta_{11},..,\eta_{31},..,\eta_{41},..]^T$. Note that $\theta_i(i=1,..,4)$ are the joint angle as shown in Fig. 2.

One can then compute the total kinetic energy K.E. and potential energy P.E. By applying Lagrange's equation with workless constraints and neglecting gravity, the dynamic differential equation becomes

$$M\begin{bmatrix} \ddot{\theta} \\ \ddot{\eta} \end{bmatrix} + \begin{bmatrix} f_1 \\ f_2 \end{bmatrix} + \begin{bmatrix} 0 & 0 \\ 0 & \bar{K} \end{bmatrix} \begin{bmatrix} \theta \\ \eta \end{bmatrix} + [\Phi_q]^T \vec{\lambda} = \begin{bmatrix} \bar{Q} \\ 0 \end{bmatrix} \qquad (2\text{-}9)$$

where M is the inertia matrix.
f_1 and f_2 are vectors including the nonlinear coupling terms of rigid body variables and flexible variables and their derivatives.
$\bar{K}$ is $\mathrm{diag}(K_{11},..,K_{31},..,K_{41}..)$ is the modal stiffness matrix.
$\bar{Q}$ is the vector of the generalized forces.
$[\Phi_q]^T$ is the constraint Jacobian matrix.
$\vec{\lambda}$ is the vector of Lagrange multipliers.

III. SINGULAR VALUE DECOMPOSITION FOR DYNAMIC ANALYSIS

Let (2-9) be expressed in the following matrix equation of order n :

$$M\ddot{q} + F + Kq + \Phi_q^T \lambda = Q \tag{3-1}$$

Note the equivalence of each term in equation (3-1) with the corresponding term in equation (2-9). Differentiating the m constraint equations (2-8) with respect to time yields

$$\Phi_q \dot{q} = 0 \tag{3-2}$$

and the initial conditions are consistent with system constraints, i.e.

$$\begin{aligned} q(t_0) &= q_0 \\ \dot{q}(t_0) &= \dot{q}_0 \end{aligned} \tag{3-3}$$

The equation (3-2) is valid because (2-8) is not an explicit function of time. Now, the mxn constraint Jacobian matrix Φ_q, with rank m, may be decomposed into the form [9]

$$\Phi_q = U \Sigma V^T \tag{3-4}$$

or, with proper partitioning proper,

$$\Phi_Q = [U_1 \; U_2] \begin{bmatrix} \Sigma_M & 0 \end{bmatrix} \begin{bmatrix} V_1^T \\ V_2^T \end{bmatrix} \tag{3-5}$$

where $u1 = \phi q \, v1 \, \sigma m\text{-}1$

$\sigma m = \text{diag}(\sigma 1, \sigma 2, .., \sigma m)$ and $\sigma 1 > \sigma 2 > .. > \sigma m$

the matrices u2 and v2 may be any matrices with orthonormal columns spanning the null spaces of ϕqt and ϕq [9]. the mxn matrix Σ in (3-4) has zeros in the last n-m columns and the σ_i's are called the singular values of matrix Φ_q. The columns of the mxm matrix U are orthonormal eigenvectors of the symmetric matrix $\Phi_q^T \Phi_q$ and σ_i^2 are the corresponding eigenvalues. The rows of nxn matrix V are also the orthonormal eigenvectors of the symmetric matrix $\Phi_q^T \Phi_q$. Therefore, V_2 satisfies the following relation:

$$\Phi_q V_2 = 0 \, , \tag{3-6}$$

and Φ_q^+ , called pseudo inverse of Φ_q, is defined as

$$\Phi_q^+ = [V_1 \;\; V_2] \begin{bmatrix} \Sigma_m^{-1} \\ 0 \end{bmatrix} \begin{bmatrix} U_1^T \\ U_2^T \end{bmatrix} \tag{3-7}$$

In what follows, an algorithm which eliminates the constraint forces from the equation of motion by imposing the condition on matrix V_2 in (3-6) will be developed. Premultiplying equation (3-1) by V_2^T gives

$$V_2^T M \ddot{q} + V_2^T F + V_2^T K q = V_2^T Q \tag{3-8}$$

where equation (3-6) has been utilized. Note that the columns of V_2 are base vectors for the null space of Φ_q.

Consequently, (3-8) is now a set of n-m equations. Let us define a new variable z which is a constraint independent coordinate with dimension n-m such that $V_2\dot{z}$ is the homogeneous solution to equation (3-2) and

$$\dot{q} = V_2 \dot{z} \tag{3-9}$$

Geometrically, it is the projection of the velocity vector $\dot{q}$ onto the tangent hyperplane of the constraint surface. The time derivative of equation (3-2) gives

$$\Phi_q \ddot{q} = -\dot{\Phi}_q \dot{q} \tag{3-10}$$

Meanwhile, $V_2\ddot{z}$ is the homogeneous solution to (3-10). Then, q can be represented below as

$$\ddot{q} = -\Phi_q^+ \dot{\Phi}_q \dot{q} + V_2 \ddot{z} \tag{3-11}$$

Physically, the first and second terms in the right hand side of (3-11) are the normal acceleration and tangential acceleration respectively. By integrating (3-9), one obtains a coordinate transformation between q and z

$$q = V_2 z + C \tag{3-12}$$

where C , a constant, is here chosen to be null to satisfy initial conditions (3-3).

Because the virtual displacement vector lies on the tangent plane of the constraint surface in a fixed time interval, the change in generalized coordinates q or independent coordinates z due to the integration does not result in a significant violation of the constraints. Hence, substituting (3-9), (3-11) and (3-12) into (3-8), the dynamic equation becomes

$$V_2^T M V_2 \ddot{z} + V_2^T F + V_2^T K V_2 z = V_2^T Q + V_2^T M \dot{\Phi}_q^+ \dot{\Phi}_q V_2 \dot{z} \tag{3-13}$$

which is a set of n-m equations in terms of the independent generalized coordinates z.

As a result, the n equations in (3-1) and m constraint equations in (2-8) are reduced to n-m equations in (3-13) by the coordinate transformation (3-2). The equations of motion can be solved by the singular value decomposition method which is efficient and stable.

IV. CONTROL SCHEME STUDIED

In this section, an alternative joint torque control for the planar motion of lightweight arms has been conducted. A control algorithm which is used in constrained dynamic systems has been developed [16]. Under this feedback control, the stability of the system in the vicinity of an operating point is considered and holonomic constraints are maintained in the state space; i.e. the control scheme implemented is satisfied only with small motion. However, the lightweight arms studied here move comparatively large distances at speeds such that the nonlinear coupling terms including centrifugal and coriolis forces become of great influence in the dynamics. Furthermore, due to the flexible nature of the lightweight structure, the position accuracy is deteriorated by structural deformation, especially when the deformation is oscillatory. Therefore, a different control scheme is used here. Furthermore, the system may require better accuracy in the response of the arm's end point to input commands to the joint control system than this simplified controller can provide [17]. However, the simplest way to reduce these vibrations is to increase the rigidity of the arm [12].

Most practical controllers use only joint position and velocity measurements. In the case of lightweight arms with flexibility, the independent joint control (IJC) which is based on a rigid model of the arm has been applied to the flexible model to satisfy the system stability [17]. However, to improve the system performance, a general rigid control (GRC) is suggested. GRC is more complex, involving feedback signal between the joints [17]. With GRC, it is feasible to explore system performance by varying all cross feedback gains independently and finding values which yield good relative pole

locations in either the flexible or the rigid model. However, sufficient design freedom does not exist for arbitrary specification of the poles and responses of the dynamic system may tend to be rather oscillatory.

The torques in (3-1) are constructed by the general rigid control which is proportional to the difference between the real and the desired signals. In other words, a joint PD (Proportional-Derivative) controller is imposed as shown below

$$Q = K_p[(\theta_{d1} - \theta_1),(\theta_{d2} - \theta_2)]^T + K_d[(\dot{\theta}_{d1} - \dot{\theta}_1),(\dot{\theta}_{d2} - \dot{\theta}_2)]^T \quad (4\text{-}1)$$

where K_p and K_d are the proportional and derivative gain matrices of dimension 2x2. θ_d is the desired value for θ. Notice that only two joint angles need to be measured for control purposes in this three link constrained system, while the flexible modes are associated with the deflection of lightweight links relative to the rigid-body rotation as illustrated in (Fig. 2).

By neglecting the actuator dynamics, the system dynamics with constraints can be transformed and reduced by the singular value decomposition. The responses of the system are then simulated with the digital computer, while the generalized force is specified by the feedback controller.

V. SIMULATIONS

Assuming that the amplitudes of the higher modes of the flexible link are very small compared to the lower modes, the system can be truncated with l equal to 2. The orthogonal shape functions which result from the boundary conditions are expressed as

$$\xi_{1j}(x) = \cos\left[\frac{\lambda_{1j}x}{L_1}\right] + \cosh\left[\frac{\lambda_{1j}x}{L_1}\right] + \gamma_{1j}\left\{\sinh\left[\frac{\lambda_{1j}x}{L_1}\right] - \sin\left[\frac{\lambda_{1j}x}{L_1}\right]\right\} \quad (5\text{-}1)$$

for the lower link with j = 1,2. The modal parameters are λ_{11}=1.158, λ_{12}=4.002 and γ_{11}=0.915, γ_{12}=1.005. For the parallel link, the shape functions are

$$\xi_{3j}(x) = \sin\left[\frac{j\pi x}{L_3}\right] \qquad j = 1,\ 2 \qquad (5\text{-}2)$$

and for the upper link,

$$\xi_{4j}(x) = \cos\left[\frac{\lambda_{4j}x}{L_4}\right] + \cosh\left[\frac{\lambda_{4j}x}{L_4}\right] + \gamma_{1j}\left\{\sinh\left[\frac{\lambda_{4j}x}{L_4}\right] - \sin\left[\frac{\lambda_{4j}x}{L_4}\right]\right\} \quad (5\text{-}3)$$

The modal parameters are λ_{41}=1.875, λ_{42}=4.694 and γ_{41}=0.734, γ_{42}=1.018.

By applying Lagrange's equation, the system dynamics (2-9) is derived in terms of the state variables that consist of 4 joint angles and 6 flexible modes, neglecting the gravitational force. Moreover, the axial elongations of the upper and parallel links are assumed negligible so that the constraint equation (2-8) yields

$$\Phi(q) = \begin{bmatrix} L_1C_1 - U_{1e}S_1 + L_2C_{14} - L_2C_{12} - L_3C_{123} \\ L_1S_1 + U_{1e}C_1 + L_2S_{14} - L_2S_{12} - L_3S_{123} \end{bmatrix} = 0 \quad (5\text{-}4)$$

where L_i is the length of the link i

$S_{ijk} = \mathrm{Sin}(\theta_i + \theta_j + \theta_k)$

$C_{ijk} = \mathrm{Cos}(\theta_i + \theta_j + \theta_k)$

$U_{1e} = \xi_{11}(L_1)\eta_{11}(t) + \xi_{12}(L_1)\eta_{12}(t)$,

while the initial conditions are chosen to be null in (3-3).

To track the desired angles from 0 to $\pi/4$ for θ_1 and θ_2 in one second, two sets of PD controller gains have been carried. One is

$$K_p = \begin{bmatrix} 554 & 138 \\ 91 & 213 \end{bmatrix} \quad K_d = \begin{bmatrix} 773 & 449 \\ 77 & 98 \end{bmatrix}, \qquad (5\text{-}5a)$$

say low gains, and the other is

$$p \begin{bmatrix} 18230 & 8540 \\ 1158 & 2614 \end{bmatrix} \quad d \begin{bmatrix} 4597 & 570 \\ 419 & 218 \end{bmatrix}, \qquad (5\text{-}5b)$$

say high gains. The objective is now to solve the responses of the system dynamics using the algorithm developed in Section III. The following steps which compute the physical coordinate q and the independent coordinate z outline the numerical method :

1) The Jacobian matrix Φ_q is factored by the singular value decomposition subroutine [19]. Then, define the independent coordinate z_i at time step i under agreement with initial conditions,

$$z_i = V_2^T q_i \qquad (5\text{-}6)$$

2) By substituting q_i into equation (3-13), the Adams Predictor-Corrector method is used to yield z_{i+1} and $\dot{z}_{i+1}$ [19]. Note that the initial conditions for equation (3-13) restart with z_i for each step.

3) Transform z_{i+1} and $\dot{z}_{i+1}$ into q_{i+1} and $\dot{q}_{i+1}$ through (3-12) and (3-9) respectively.

4) Check the tolerance of the constraint violation. If $||\dot{z}||^2$ is beyond the criterion of $||\dot{q}||^2$ by a prescribed value (chosen here to be 0.01), the Jacobian matrix Φ_q needs to be redecomposed [9] and step 1) repeated. Otherwise, step 2) is executed next.

Repeat the above steps, until the final time is reached. The time interval is chosen as 5 msec. Fig. 3 to Fig. 9 show the feedback control results. Obviously, the joint responses (Fig. 3 - Fig. 4) of high gains have better tracking than those of low gains, while both converge to the desired final position in the steady state. The end point error of the structure with respect to the rigid-body motion goes to zero as shown in Fig. 5. Fig. 6 and Fig. 7 demonstrate the tolerance of $||\Phi(q)||$ and $||\Phi_q\dot{q}||$ to the time history individually. The tolerance of $||\Phi(q)||$ for high gains is found to be larger than for low gains, but still an acceptable magnitude of order 10^{-5}. Furthermore, $\Phi_q\dot{q}$ shows a tolerance of order 10^{-7} for both gains in Fig. 7. The input torques are shown in Fig. 8 and Fig. 9.

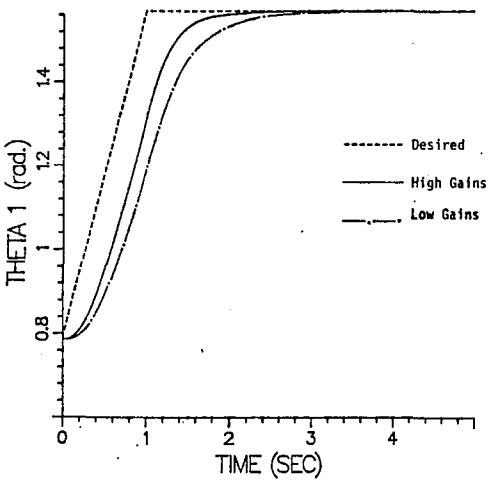

Figure 3. The responses of the first joint angle.

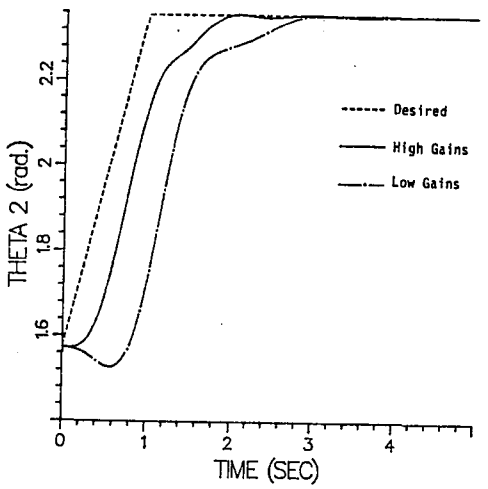

Figure 4. The responses of the second joint angle.

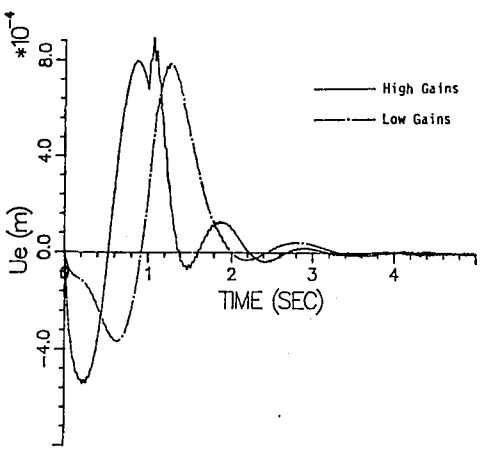

Figure 5. The responses of the end point error.

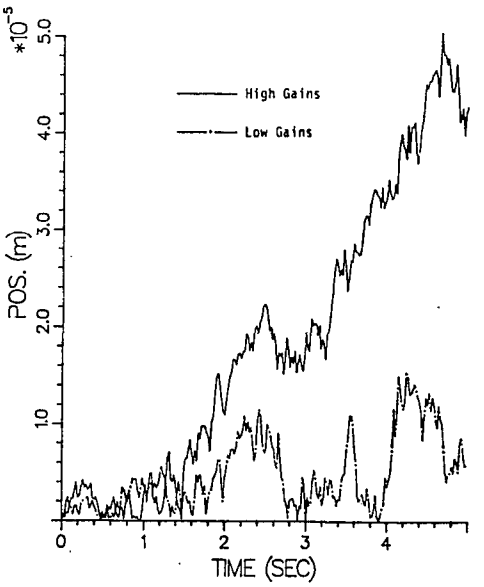

Figure 6. The tolerance for the constraint $\Phi(q)$.

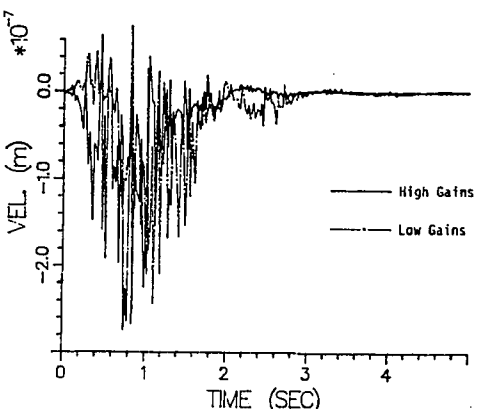

Figure 7. The tolerance for the time derivative $\Phi_q \dot{q}$ of the constraint.

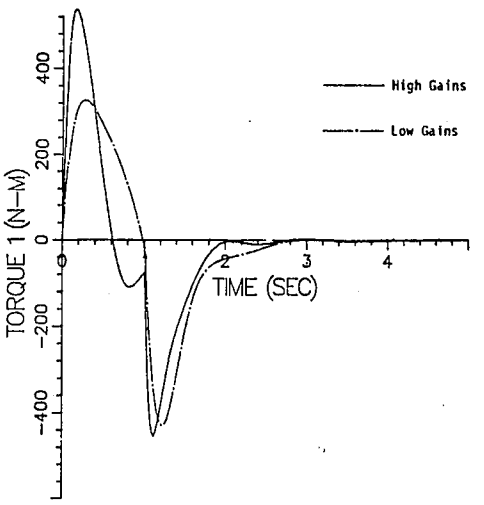

Figure 8. The responses of the first joint control torque.

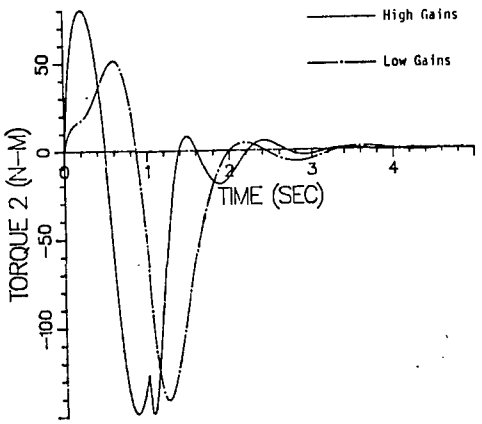

Figure 9. The responses of the second joint control torque.

VI. CONCLUSIONS

A dynamic model for a lightweight arm with a parallel mechanism has been established with a constraint equation. By applying the singular value decomposition to the Jacobian matrix of the constraint, a transformation between the physical and the independent coordinates is obtained. Because of nullspace characteristics in the transformation and the Jacobian, the equation of motion is reduced to state space form in the independent coordinates without workless constraint forces. A general rigid joint controller has been suggested to meet the practical operation in this study. However, advanced control algorithms for a constrained system with large motion needs to be investigated further. The updating method which evaluates the constraint violation and then maintains nullspace continuity illustrates the numerical stability and efficiency of the SVD algorithm.

VII. ACKNOWLEDGEMENTS

The authors would like to acknowledgement that this material is based in part on work supported by the Computer Integrated Manufacturing Systems (CIMS) at Georgia Tech, and by Grant #NAG-1-623 of the National Aeronautics and Space Administration.

REFERENCES

[1] Book, W.J., "New Concepts in Lightweight Arms", 2nd International Symposium on Robotic Research, 1985.

[2] Hastings, G.,G., "Controlling Flexible Manipulators; An Experimental Investigation," Ph.D. Thesis, School of Mechanical Engineering, Georgia Institute of Technology. 1986.

[3] Cannon,R.M., and Schmitz,E., "Initial Experiments on The End-Point Control of a Flexible One-Link Robot," The International Journal of Robotics Research, Fall 1984.

[4] Book,W.J., Le,S., and Sangveraphunsiri,V., "The Bracing Strategy for Robot Operation," CISM-IFToMM Symposium on Robots and Manipulators (RoManSy), 1984.

[5] Maizza-Neto,O., "Modal Analysis and Control of Flexible Manipulator Arms", Ph.D. thesis,Department of Mechanical Engineering, M.I.T., Sept. 1974.

[6] Greenwood,D.T., Principles of Dynamics, Prentice-Hall Inc, 1965.

[7] Nikravesh, P.E, "Some Methods for Dynamic Analysis of Constrained Mechanical System: A Survey", Computer Aided Analysis and Optimization of Mechanical System Dynamics, E.J.Haug, ed., Springer-Verlag, Heidelberg, West Germany, 1984.

[8] Hemani,H., Jaswa,V.C., and McGhee,R,B., "Some Alternative Formulations of Manipulator Dynamics for Computer Simulation Studies," Allerton Conference on Circuit and System Theory, 1975.

[9] Mani,N.K., Haug,E.J, and Atkinson,K.E., "Application of Singular Value Deconposition for Analysis of Mechanical System Dynamics", ASME Journal of Mechanisms, Transmissions, and Automation in Design, 107, March 1985.

[10] Singh,R.P., and Linkins, P.W., "Singular Value Decomposition for Constrainted Dynamic Systems", ASME Journal of Applied Mechanics, 52(4), Dec. 1985.

[11] Hemani,H., and Wyman,B.F., "Indirect Control of The Forces of Constraint in Dynamic Systems," ASME Journal of Dynamic Systems, Measurement, and Control, 1979.

[12] Book,W.J., "Modeling,Design and Control of Flexible Manipulator Arms",Ph.D. thesis,Department of Mechanical Engineering, M.I.T., Apr. 1974.

[13] Meirovitch,L., Elements of Vibration Analysis, McGraw-Hill Inc, 1975.

[14] Huggins,J.D., Kwon,D.S., Lee,J.W., and Book,W.J., "Alternative Modeling and Verification Techniques for a Large Flexible Arm," Conference on Applied Motion Control, 1987.

[15] Kim, S.S., Vanderploeg, M.J., "QR Decomposition for State Space Representation of Constrained Mechanical Dynamic Systems", ASME Journal of Mechanisms, Transmissions, and Automation in Design, 108, June 1986.

[16] Hemani,H.,and Wyman,B.F., "Modeling and Control of Constrained Dynamic Systems with Application to Biped Locomotion in The Frontal Plane," IEEE Trans. on Automatic Control, 1979.

[17] Book,W.F., Maizza-Neto,O., and Whitney,D.E., "Feedback and Control of Two Beam, Two Joint Systems with Distributed Flexibility," ASME Journal of Dynamic Systems, Measurement, and Control, 1975.

[18] Hasting,G.G., and Book, W.J., "A linear Dynamic Model for Flexible Robotic Manipulators," IEEE Control Systems Magazine, 1987.

[19] IMSL Reference Mannual, International Mathematical and Statistical Libraries Inc., Huston,Tx.